Available online at www.sciencedirect.com
SCIENCE DIRECT®
Tetrahedron Letters 46 (2005) 3917–3921
Tetrahedron Letters

Spectroscopic and DFT evidence for a nonclassical radical cation derived from 7-benzhydrylidenenorbornene

Hiroshi Ikeda,[a,*] Hayato Namai[a] and Takashi Hirano[b]

[a]*Department of Chemistry, Graduate School of Science, Tohoku University, Sendai 980-8578, Japan*
[b]*Department of Applied Physics and Chemistry, The University of Electro-Communications, Chofu, Tokyo 182-8585, Japan*

Received 16 February 2005; revised 14 March 2005; accepted 18 March 2005
Available online 11 April 2005

Abstract—Nanosecond time-resolved UV/vis absorption spectroscopy on laser flash photolysis was conducted for photoinduced electron-transfer reactions of 7-benzhydrylidenenorbornene (**1**) and 7-benzhydrylidenenorbornane (**5**). The differences in the observed absorption bands and the structures of $\mathbf{1}^{\cdot+}$ and $\mathbf{5}^{\cdot+}$ were evaluated successfully using calculations based on (time dependent) density functional theory, confirming the nonclassical nature of $\mathbf{1}^{\cdot+}$.
© 2005 Elsevier Ltd. All rights reserved.

Previously, Hirano, Ohashi and co-workers reported[1,2] the π-facial selective nucleophilic addition to the radical cation of 7-benzhydrylidenenorbornene (**1**, Scheme 1, anodic peak potential = +1.50 V vs SCE in acetonitrile), triggered by a photoinduced electron-transfer (PET) reaction using a sensitizer. The π-facial selectivity was explained by the possible generation of a nonclassical radical cation ($\mathbf{1}^{\cdot+}$) involved with electronic coupling of exocyclic (C-7–C-8) and endocyclic (C-2–C-3) double bonds. It was suspected that nucleophilic attack of a methanol or water molecule to $\mathbf{1}^{\cdot+}$ preferentially occurs from the *anti* side of the endocyclic double bond. Unfortunately, however, $\mathbf{1}^{\cdot+}$ was not observed directly. If $\mathbf{1}^{\cdot+}$ are observed using UV/vis absorption spectroscopy, it will be of value, because such electronic coupling was recognized as a homoconjugation and has been suggested to play a crucial role in electron-transfer reactions of 7-methylenenorbornadiene (**3**)[3] and 7-methylenequadricyclane (**4**),[3]

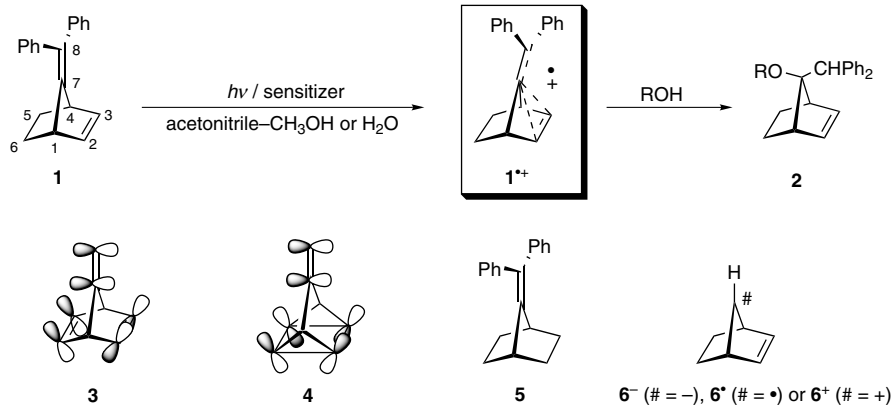

Scheme 1. Top: possible generation of a nonclassical radical cation ($\mathbf{1}^{\cdot+}$) in the PET π-facial selective nucleophilic addition reaction of **1**. Bottom: a list of related compounds (**3**–**5** and $\mathbf{6}^{\#}$).

Keywords: Photochemistry; Nonclassical radical cation; π-Facial selectivity; Absorption spectra; Electronic coupling.
* Corresponding author. Fax: +81 22 795 6557; e-mail: ikeda@org.chem.tohoku.ac.jp

0040-4039/$ - see front matter © 2005 Elsevier Ltd. All rights reserved.
doi:10.1016/j.tetlet.2005.03.156

and has only been detected by CIDNP.[4] Therefore, we studied nanosecond time-resolved UV/vis absorption spectroscopy on laser flash photolysis (LFP) of **1** and structurally related 7-benzhydrylidenenorbornane[2] (**5**, Scheme 1). Here, we report the direct observation of a nonclassical radical cation $\mathbf{1}^{\bullet+}$ together with the results of density functional theory (DFT) and time-dependent (TD) DFT calculations.

Nanosecond time-resolved UV/vis absorption spectroscopy on LFP[5] was performed with *N*-methylquinolinium tetrafluoroborate ($NMQ^+BF_4^-$) and toluene as a sensitizer and a cosensitizer,[6] respectively, in aerated acetonitrile at 298 K. As shown in Figure 1a and b, laser excitation (355 nm) of $NMQ^+BF_4^-$ with **1** in aerated acetonitrile gave an intense sharp absorption band with λ_{ab} at 391 nm (band A), a broad weak absorption band at 480–580 nm (band B), and a broad intense absorption band at 600–850 nm (band C).[7] The differential optical densities (ΔOD) observed at 391, 560, and 750 nm decreased synchronously with almost the same rate constant, $k_d \sim 7 \times 10^5\ s^{-1}$, indicating that these bands originate in the same species, $\mathbf{1}^{\bullet+}$. Similarly, $\mathbf{5}^{\bullet+}$ had three bands: a sharp intense absorption band with λ_{ab} at 386 nm (band A′), a broad weak absorption band at 500–650 nm (band B′), and a broad intense absorption band at >700 nm (band C′) (Fig. 1c and d).[7] Interestingly, the λ_{ab} (391 nm) of band A of $\mathbf{1}^{\bullet+}$ was redshifted slightly, compared with that (386 nm) of band A′ of $\mathbf{5}^{\bullet+}$, while a large blueshift was observed for the λ_{ab} (600–850 nm) of band C of $\mathbf{1}^{\bullet+}$ as compared to that (>700 nm) of band C′ of $\mathbf{5}^{\bullet+}$.

To gain insight into the electronic structure of $\mathbf{1}^{\bullet+}$, we performed DFT calculations[8] for **1**, $\mathbf{1}^{\bullet+}$, **5**, and $\mathbf{5}^{\bullet+}$. As shown in Figure 2a, the subunit of the exocyclic double bond in the neutral **1** bends slightly toward the C-5–C-6 methylene side at the B3LYP/cc-pVDZ level. Conversely, $\mathbf{1}^{\bullet+}$ is calculated to bent in the opposite manner, as shown in Figure 2b. The C-1–C-7–C-4 skeleton and the exocyclic double bond of $\mathbf{1}^{\bullet+}$ bend to the side of the endocyclic double bond by 5.2° [=(360.0° − 115.0°)/2 − 117.3°] and 5.0° (=180.0° − 175.0°), respectively, at the UB3LYP/cc-pVDZ level. Note that the calculation suggests a symmetrical structure for **5** and $\mathbf{5}^{\bullet+}$, the structurally related species without an endocyclic double bond (Fig. 2d and e).

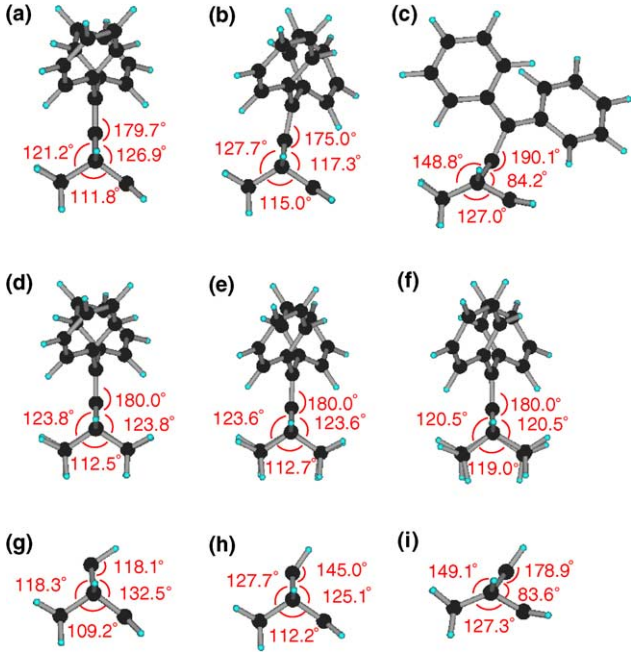

Figure 2. Side views of **1** (a), $\mathbf{1}^{\bullet+}$ (b), $\mathbf{1}^{2+}$ (c), **5** (d), $\mathbf{5}^{\bullet+}$ (e), $\mathbf{5}^{2+}$ (f), $\mathbf{6}^-$ (g), $\mathbf{6}^{\bullet}$ (h), and $\mathbf{6}^+$ (i) optimized using the (U)B3LYP/(aug-)cc-pVDZ calculations.

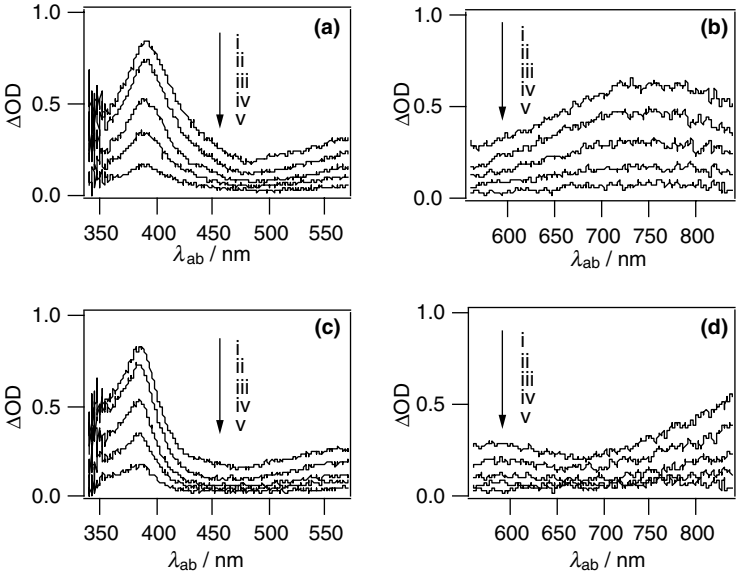

Figure 1. Nanosecond time-resolved UV/vis absorption spectra observed in the LFP of **1** (a and b, 1 mM) and **5** (c and d, 1 mM) under $NMQ^+BF_4^-$ (10 mM)–toluene (1 M)-sensitized conditions in aerated acetonitrile. Spectra (i) 100 ns, (ii) 400 ns, (iii) 1 μs, (iv) 2 μs, and (v) 5 μs.

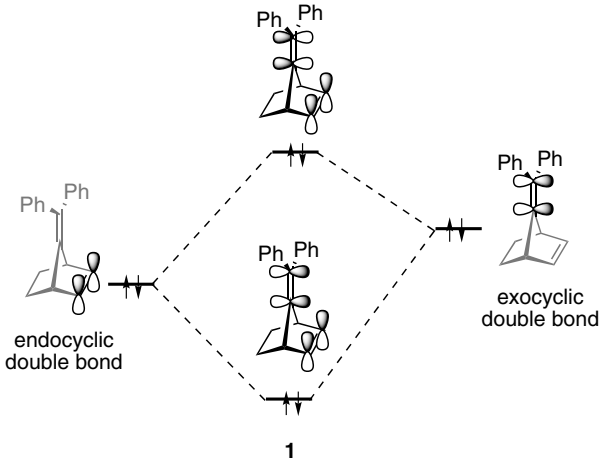

Figure 3. Conceptual representation showing the orbital interaction between the exocyclic and endocyclic double bonds in **1**.

The bent structure of **1** is owing to a dominant antibonding orbital interaction between the exocyclic and endocyclic double bonds, as shown in Figure 3: the existence of two electrons in the HOMO, which is composed of an antibonding combination of exocyclic and endocyclic double bonds, contributes the bent of the exomethylene toward the C-5–C-6 methylene side in **1**.[11] Judging from the close resemblance in the MOs of **1** and $\mathbf{1}^{\cdot+}$, as exemplified by the HOMO of **1** and the SOMO (α) of $\mathbf{1}^{\cdot+}$ (Fig. 4), a similar orbital interaction operates in $\mathbf{1}^{\cdot+}$. Therefore, the loss of an electron from the HOMO of **1** induces a decreasing repulsive interaction, but does not induce an increasing attractive interaction, between the two double bonds, resulting in the bent of the exomethylene of $\mathbf{1}^{\cdot+}$ toward the C-2–C-3 methylene side. Note that the two orbitals at C-2(3) and C-7 of the HOMO of **1** are out of phase with each other, as shown in Figures 3 and 4. In evidence, the hypothetical dication $\mathbf{1}^{2+}$ bends more significantly, while the corresponding $\mathbf{5}^{2+}$ keeps a symmetric structure (Fig. 2c and f).

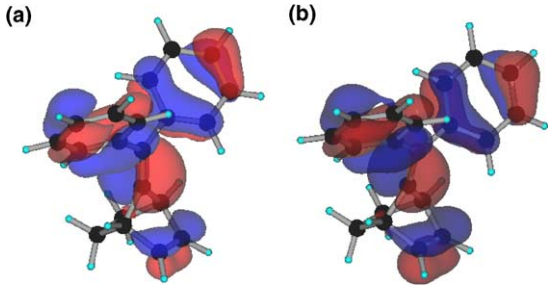

Figure 4. The HOMO of **1** (a) and SOMO (α) of $\mathbf{1}^{\cdot+}$ (b) calculated using (U)B3LYP/cc-pVDZ.

Table 1 shows the partial spin (ρ) and charge (q) density for each carbon from C-1 to C-8 of $\mathbf{1}^{\cdot+}$ and $\mathbf{5}^{\cdot+}$ together with the differences between $\mathbf{1}^{\cdot+}$ and $\mathbf{5}^{\cdot+}$. Note that ρ at C-7 (+0.326) and C-2 (+0.081) or C-3 (+0.081) of $\mathbf{1}^{\cdot+}$ decrease and increase most significantly, respectively, of all carbons of $\mathbf{1}^{\cdot+}$, compared with $\mathbf{5}^{\cdot+}$ [C-7 (+0.409) and C-2 (+0.017) or C-3 (+0.014)]. Strangely enough, q does not increase at C-2 (+0.080) and C-3 (+0.065), but increases at C-1 (−0.057) and C-4 (−0.054) of $\mathbf{1}^{\cdot+}$, compared with $\mathbf{5}^{\cdot+}$ [C-7 (+0.109), C-2 (+0.070), C-3 (+0.057), C-1 (−0.091), and C-4 (−0.091)], although q at C-7 (+0.090) of $\mathbf{1}^{\cdot+}$ is reduced significantly. This suggests that the positive charge of $\mathbf{1}^{\cdot+}$ is not always delocalized significantly over the endocyclic double bond subunit, whereas the spin is delocalized there. Note, however, that further discussion only using the ρ or q values of each carbon is misleading because spin and charge distribute not only to carbons but also to protons. Therefore, it is reasonable to compare the sum of the ρ or q values between any appropriate subunits in $\mathbf{1}^{\cdot+}$ and $\mathbf{5}^{\cdot+}$. Figure 5 clearly shows the change in the electronic structure between $\mathbf{1}^{\cdot+}$ and $\mathbf{5}^{\cdot+}$. The sum of the ρ and q values, $\sum\rho$ = +0.867 and $\sum q$ = +0.619, of the benzhydrylidene subunit in $\mathbf{1}^{\cdot+}$ decrease, as compared to those of $\mathbf{5}^{\cdot+}$, +0.968 and +0.678. Accordingly, the values of the residual subunit (+0.133 and +0.381) increase, compared with those of $\mathbf{5}^{\cdot+}$ (+0.032 and +0.322). These findings indicate that spin and charge in $\mathbf{1}^{\cdot+}$ are delocalized not only to the benzhydrylidene subunit, but also to the residual subunit. Unexpectedly, the changes in ρ and q are not very significant, as would be expected from the π-selective nucleophilic addition.[1,2] This may be attributable to the fact that $\mathbf{1}^{\cdot+}$ still possesses one electron in the SOMO with an antibonding character. From this perspective, $\mathbf{1}^{\cdot+}$ is compared to the radical $\mathbf{6}^{\cdot}$ (Scheme 1), but not to the nonclassical cation $\mathbf{6}^{+}$, because $\mathbf{6}^{\cdot}$ also has one electron in the SOMO with an antibonding

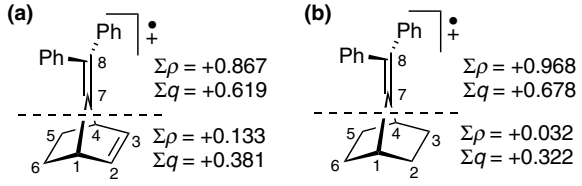

Figure 5. The sum of the partial spin (ρ) and charge (q) density of the benzhydrylidene subunit and residual subunit in $\mathbf{1}^{\cdot+}$ (a) and $\mathbf{5}^{\cdot+}$ (b) calculated using UB3LYP/cc-pVDZ.

Table 1. The partial spin (ρ) and charge (q) density in $\mathbf{1}^{\cdot+}$ and $\mathbf{5}^{\cdot+}$ calculated using TD UB3LYP/cc-pVDZ

	C-1	C-2	C-3	C-4	C-5	C-6	C-7	C-8
ρ ($\mathbf{1}^{\cdot+}$)	−0.015	+0.081	+0.081	−0.012	0.000	−0.001	+0.326	+0.145
ρ ($\mathbf{5}^{\cdot+}$)	−0.019	+0.017	+0.014	−0.019	+0.017	+0.014	+0.409	+0.090
ρ ($\mathbf{1}^{\cdot+}$) − ρ ($\mathbf{5}^{\cdot+}$)	+0.004	+0.064	+0.067	+0.007	−0.017	−0.015	−0.083	+0.055
q ($\mathbf{1}^{\cdot+}$)	−0.057	+0.080	+0.065	−0.054	+0.081	+0.070	+0.090	+0.056
q ($\mathbf{5}^{\cdot+}$)	−0.091	+0.070	+0.057	−0.091	+0.070	+0.057	+0.109	+0.034
q ($\mathbf{1}^{\cdot+}$) − q ($\mathbf{5}^{\cdot+}$)	+0.034	+0.010	+0.008	+0.037	+0.011	+0.013	−0.019	+0.022

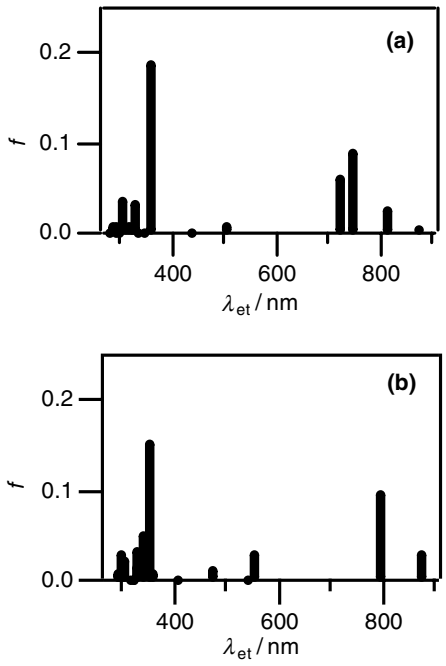

Figure 6. Electronic transitions of $\mathbf{1}^{\cdot+}$ (a) and $\mathbf{5}^{\cdot+}$ (b) calculated using TD UB3LYP/cc-pVDZ.

character. Similar structural changes are found in the series **1**, $\mathbf{1}^{\cdot+}$, and $\mathbf{1}^{2+}$ and the series $\mathbf{6}^{-}$, $\mathbf{6}^{\cdot}$, and $\mathbf{6}^{+}$ (Fig. 2g–i).

The electronic transition wavelengths (λ_{et}) and oscillator strengths (f) of $\mathbf{1}^{\cdot+}$ and $\mathbf{5}^{\cdot+}$ in the optimized structures were calculated using TD UB3LYP/cc-pVDZ and are shown in Figure 6. The calculated λ_{et} at 362, 506, 724, 751, and 817 nm with $f = 0.187$, 0.009, 0.059, 0.087, and 0.024 for $\mathbf{1}^{\cdot+}$ are in agreement with the observed UV/vis absorption spectra (Fig. 1a and b) of $\mathbf{1}^{\cdot+}$ on LFP. Similarly, the 353, 554, 800, and 878 nm transitions with $f = 0.153$, 0.027, 0.094, and 0.028 calculated as the λ_{et} of $\mathbf{5}^{\cdot+}$, are in line with the UV/vis absorption spectra (Fig. 1c and d) of $\mathbf{5}^{\cdot+}$. The red- and blueshift of λ_{ab} of $\mathbf{1}^{\cdot+}$ as compared to that of $\mathbf{5}^{\cdot+}$ are reproduced successfully in the TD DFT calculation, confirming the electronic coupling between the two double bonds in $\mathbf{1}^{\cdot+}$ and the generation of a nonclassical radical cation, $\mathbf{1}^{\cdot+}$.

In conclusion, we observed a nonclassical radical cation $\mathbf{1}^{\cdot+}$[1,2,13] by nanosecond time-resolved UV/vis absorption spectroscopy on LFP. The electronic coupling[15] in $\mathbf{1}^{\cdot+}$ is based on an orbital interaction between exocyclic and endocyclic double bonds. The DFT and TD DFT calculations suggest the bent structure of $\mathbf{1}^{\cdot+}$ owing to the electronic coupling and support the red- and blueshift of the absorption spectra of $\mathbf{1}^{\cdot+}$ as compared to those of $\mathbf{5}^{\cdot+}$ having no electronic coupling. The degree of delocalization of spin and charge to the endocyclic double bond in $\mathbf{1}^{\cdot+}$ is relatively small. Therefore, careful consideration is needed to judge whether the electronic coupling causes the π-selectivity[1,2] observed in the PET nucleophilic addition reaction of **1**. Further studies for this subject and to characterize the reactivity of $\mathbf{1}^{\cdot+}$ are now in progress, and will be published elsewhere.

Acknowledgements

H.I. gratefully acknowledges financial support from a Grant-in-Aid for Scientific Research on Priority Areas (no. 417) from the Ministry of Education, Culture, Sports, Science, and Technology of Japan (no. 14050008). We also thank Professors M. Ueda (Tohoku University) and H. Niwa (UEC) for their generous considerations, and Dr. H. Ishii (UEC) and the late Mr. S. Shiina (UEC) for their efforts in preparing the samples.

Supplementary data

Supplementary data associated with this article can be found in the online version, at doi:10.1016/j.tetlet.2005.03.156. The DFT calculation results for **1**, $\mathbf{1}^{\cdot+}$, $\mathbf{1}^{2+}$, **5**, $\mathbf{5}^{\cdot+}$, $\mathbf{5}^{2+}$, $\mathbf{6}^{-}$, $\mathbf{6}^{\cdot}$, and $\mathbf{6}^{+}$, the absorption spectra of *n*-butyl chloride glassy matrices of **1** and **5** obtained after irradiation with γ-rays at 77 K, and the definition of the angles shown in Figure 2 (PDF). This material is available free of charge via the Internet at http://www.sciencedirect.com.

References and notes

1. Hirano, T.; Shiina, S.; Ohashi, M. *J. Chem. Soc., Chem. Commun.* **1992**, 1544–1546.
2. Ishii, H.; Shiina, S.; Hirano, T.; Niwa, H.; Ohashi, M. *Tetrahedron Lett.* **1999**, *40*, 523–526.
3. Weng, H.; Du, X.-M.; Roth, H. D. *J. Am. Chem. Soc.* **1995**, *117*, 135–140.
4. Roth, H. D.; Du, X.-M.; Weng, H.; Lakkaraju, P. S.; Abelt, C. J. *J. Am. Chem. Soc.* **1994**, *116*, 7744–7752.
5. Nanosecond time-resolved UV/vis absorption spectroscopy on LFP was carried out with a pulsed YAG laser (Continuum Surelite-10, Nd, THG, λ_{ex} = 355 nm, 55 mJ) using a Xe arc lamp (150 W) as the monitoring light. The region of the observable wavelength in the multichannel experiment is 280 nm wide. Therefore, we observed the absorption spectra in the 310–590 and 560–840 nm regions separately.
6. The use of cationic sensitizers and chemically unreactive aromatic hydrocarbons, so-called cosensitizers, in acetonitrile is effective for observing radical cations in LFP experiments. Under cosensitized conditions, a substrate radical cation is formed via electron transfer from a cosensitizer to a photoexcited sensitizer followed by hole transfer from a cosensitizer radical cation to the substrate.
7. Similar absorption bands were observed in an *n*-butyl chloride glassy matrix of **1** and **5** irradiated with γ-rays at 77 K. See the Supplementary Data.
8. DFT and TD DFT calculations were performed using the program Gaussian 98.[9] Figures 2 and 4 were drawn using the MolStudio software.[10]
9. Frisch, M. J.; Trucks, G. W.; Schlegel, H. B.; Scuseria, G. E.; Robb, M. A.; Cheeseman, J. R.; Zakrzewski, V. G.; Montgomery, J. A.; Stratmann, R. E.; Burant, J. C.; Dapprich, S.; Millam, J. M.; Daniels, A. D.; Kudin, K. N.; Strain, M. C.; Farkas, O.; Tomasi, J.; Barone, V.; Cossi, M.; Cammi, R.; Mennucci, B.; Pomelli, C.; Adamo, C.;

Clifford, S.; Ochterski, J.; Petersson, G. A.; Ayala, P. Y.; Cui, Q.; Morokuma, K.; Malick, D. K.; Rabuck, A. D.; Raghavachari, K.; Foresman, J. B.; Cioslowski, J.; Ortiz, J. V.; Stefanov, B. B.; Liu, G.; Liashenko, A.; Piskorz, P.; Komaromi, I.; Gomperts, R.; Martin, R. L.; Fox, D. J.; Keith, T.; Al-Laham, M. A.; Peng, C. Y.; Nanayakkara, A.; Gonzalez, C.; Challacombe, M.; Gill, P. M. W.; Johnson, B. G.; Chen, W.; Wong, M. W.; Andres, J. L.; Head-Gordon, M.; Replogle, E. S.; Pople, J. A. *Gaussian 98* (*Revision A.11.4*), Gaussian, Inc., Pittsburgh, PA, 1998.

10. For MolStudio (NEC), visit the web site at http://www.sw.nec.co.jp/APSOFT/SX/molstudio_e/index.html.
11. A similar orbital interaction between exocyclic and endocyclic double bonds was confirmed using photoelectron spectroscopy for isopropylidenenorbornene. See Ref. 12.
12. Heilbronner, E.; Martin, H.-D. *Helv. Chim. Acta* **1972**, *55*, 1490–1502.
13. For recent studies of nonclassical cations, see Ref. 14 and the references cited therein.
14. Laube, T. *J. Am. Chem. Soc.* **2004**, *126*, 10904–10912.
15. For further suggestions of similar electronic coupling through space and bond in reactive radical cations, see Ref. 16.
16. (a) Ikeda, H.; Hoshi, Y.; Kikuchi, Y.; Tanaka, F.; Miyashi, T. *Org. Lett.* **2004**, *6*, 1029–1032; (b) Ikeda, H.; Hoshi, Y.; Miyashi, T. *Tetrahedron Lett.* **2001**, *42*, 8485–8488; (c) Ikeda, H.; Takasaki, T.; Takahashi, Y.; Konno, A.; Matsumoto, M.; Hoshi, Y.; Aoki, T.; Suzuki, T.; Goodman, J. L.; Miyashi, T. *J. Org. Chem.* **1999**, *64*, 1640–1649; (d) Ikeda, H.; Minegishi, T.; Abe, H.; Konno, A.; Goodman, J. L.; Miyashi, T. *J. Am. Chem. Soc.* **1998**, *120*, 87–95; (e) Brede, O.; David, F.; Steenken, S. *J. Chem. Soc., Perkin Trans. 2* **1995**, 23–32; (f) Williams, F. *J. Chem. Soc., Faraday Trans.* **1994**, *90*, 1681–1687; (g) Tamai, T.; Mizuno, K.; Hashida, I.; Otsuji, Y. *J. Org. Chem.* **1992**, *57*, 5338–5342; (h) Tojo, S.; Toki, S.; Takamuku, S. *J. Org. Chem.* **1991**, *56*, 6240–6243; (i) Pac, C. *Pure Appl. Chem.* **1986**, *58*, 1249–1256.